Clim. Past Discuss., 5, C172–C182, 2009
www.clim-past-discuss.net/5/C172/2009/

Climate of the Past Discussions

Interactive comment on "High resolution cyclostratigraphy of the early Eocene – new insights into the origin of the Cenozoic cooling trend" *by* T. Westerhold and U. Röhl

T. Westerhold and U. Röhl

tho@uni-bremen.de

Received and published: 9 May 2009

Reply to Interactive comment of J. Dinarès-Turell (Referee) on "High resolution cyclostratigraphy of the early Eocene – new insight into the origin of the Cenozoic cooling trend" by T. Westerhold and U. Röhl

We thank the referee for his time and effort to evaluate our discussion paper and are feel very encouraged about the positive response. However, here we reply to the points raised to even strengthen the case of a good and reliable time model:

Regarding suggestion 1: The referee asked to plot magnetic susceptibility (MS) and XRF Fe data all against the mbsf, ship composite depth (mcd) and the revised com-

posite depth (rmcd) for evaluation of the usefulness of the high resolution XRF technique. We provide these data by adding new supplementary Figures S2A, S2B, S2C, S3A, S3B, and S3C. Figures S2A, S2B, and S2C show the shipboard MS record used for the ship splicing. Figures S3A, S3B, and S3C show the new high-resolution XRF core scanning Fe data. We mark the changes between mcd and rmcd (yellow) in the figures. Studying the figures in detail reveals that the high quality XRF core scanning data with its high signal to noise ratio provide much more reliable information for the splicing process than MS data. Some of the ambiguity of the ship splice can be clearly identified, e.g., for the upper 50 meters (see Figure S2A and S3A). However, neither MS nor XRF data do show a good match using the ship offset table around 40 mcd. But readjustment of the depths applying new XRF data based correlations provides a composite section which is 4m shorter than the shipboard splice, and reveals that MS data for Holes 1258A and 1258B are very different. Another example at 62 m mcd exhibits that MS data clearly mismatch between holes. In fact, XRF data show that the bottom of Core 1258B-6R and the top of Core 1258B-7R overlap by a few decimeter. We are confident that these examples clearly demonstrate that XRF data were essential in revising the splice for Site 1258.

Regarding suggestion 2: We feel that there is a need to further clarify the magnetostratigraphy of Site 1258: The reversal pattern is well resolved but there is inconsistency in the interpretation of the polarity pattern between Holes 1258A and 1258B after adjustment to mcd between lower Chron 23n ($\sim$100 mcd) and C22n ($\sim$50 mcd) (Suganuma and Ogg, 2006). We have revised the former Figure S2 (= now Figure S4), to show both the original interpretation by Suganuma and Ogg (2006) and the interpretation used in our study. The interpretation of Suganuma and Ogg (2006) resulted from the comparison of sedimentary features based on magnetic susceptibility data and biostratigraphic datums. In particular, the offset of foraminifer Zone P8/P7 near the top of the "distorted" C23n was interpreted to result from a possible unrecognized fault in Hole 1258A which might have truncated the uppermost part of C23n in Hole 1258B and/or truncated the overlying Chron 22r in Hole 1258A. In addition the occurrence

of Orthorhabdus tribrachiatus in cores 1258B-7R and -8R was interpretated reworked (as this would be in line with the interpretation), as they were found well above the datum for the base of planktonic foraminifer Zone P9 (Shipboard Scientific Party, 2004). Following this interpretation the normal polarity interval at 80 mcd (see Figure S4b) at each site has been flagged as a pervasive overprint because it lies between C22n and C23n (see also Figure F5 in Suganuma and Ogg 2006). These anomalous normal polarities lead Suganuma and Ogg (2006) to the conclusion that either the upper part of the section was not effectively demagnetized or a hypothetical fault duplicated some portion of the record. This interpretation of Suganuma and Ogg (2006) needs to be revised as updated nannofossil datums are available. We have plotted the shipboard nannofossil datums in Figure S4 and assume that the recalibrated nannofossil events (Agnini et al. 2006; Agnini et al. 2007) are more reliable than the planktonic foraminifera zonation of Berggren et al. (1995). According to Agnini et al. (2006) the LO (Lowest Occurrence) of N. fulgens is in the mid portion of magnetochron C21n, the HO (Highest Occurrence) of D. lodoensis is in C21r, and the HO of T. orthostylus is close to the base of 22r. The LO of D. lodoensis is close to the top of C24n (Agnini et al. 2006), the LO of S. radians is in the lower portion of C24n (Agnini et al. 2006), and the LO of T. orthostylus is close to the top of C24r (Agnini et al. 2007). Based on this data the normal chron described as a pervasive overprint from 68 to 78 rmcd must be C23n. The normal polarity from $\sim$100 to $\sim$128 rmcd would be assigned to C24n. This then leads to the interpretation as given in Table S6 and used in this study. The excellent matching of XRF Fe data which refined the splice does not allow moving cores to align the reversal boundary at $\sim$84 rmcd in Hole 1258A with the boundary at $\sim$94 rmcd. At $\sim$84 rmcd in Hole 1258A the color of the cores changes from red to gray suggesting geochemical changes in the sediment. We therefore interpreted the reversal boundary at $\sim$94 rmcd in Hole 1258B in accordance with the nannofossil datum positions as the top of C24n rather then the reversal in at $\sim$84 rmcd in Hole 1258A.

Regarding suggestion 3: We agree that distinct bands in the wavelet plots are no easy to spot for both the 100 and 405 kyr bands. Therefore we have marked the 100 kyr

(dashed line) and 405 kyr (solid line) in the supplementary figure S3. The dominant cycle in our record is orbital precession, which stands out in all the plots and we feel that there is no need to especially mark this orbital frequency by a line. The well-developed precession cycles with a high amplitude resulting into small wavelet power to the modulating eccentricity. The cross-hatched cone of influence is given by the applied software of Torrence and Compo. Therefore it is apparent that we have performed the analysis to the length of the particular presented time-series and padded the edges as assumed by the referee.

Interactive comment on Clim. Past Discuss., 5, 495, 2009.

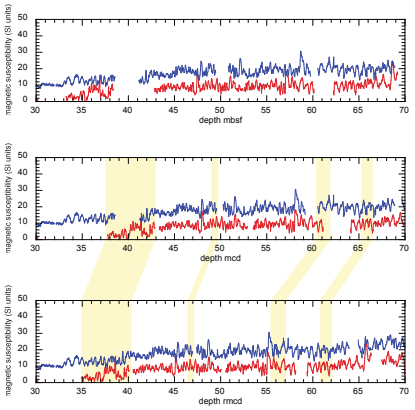

Figure S2A. Magnetic susceptibility (MS) of holes 1258A (red) and 1258B (blue) plotted along shipboard mbsf (top panel), shipboard composite depth (mcd, middle panel), and revised composite depth (rmcd, lower panel). The yellow shaded areas highlight major changes between mcd and rmcd. Note: MS values of Hole 1258B are offset by 10 units for clarity.

Fig. 1.

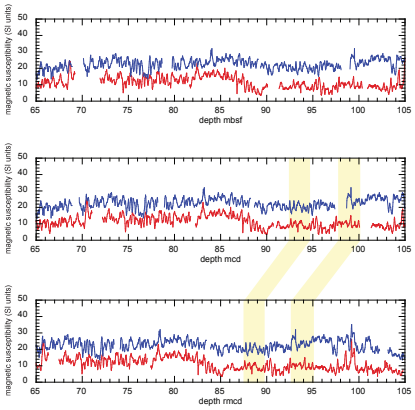

Figure S2B. Magnetic susceptibility (MS) of holes 1258A (red) and 1258B (blue) plotted along shipboard mbsf (top panel), shipboard composite depth (mcd, middle panel), and revised composite depth (rmcd, lower panel). The yellow shaded areas highlight major changes between mcd and rmcd. Note: MS values of Hole 1258B are offset by 10 units for clarity.

Fig. 2.

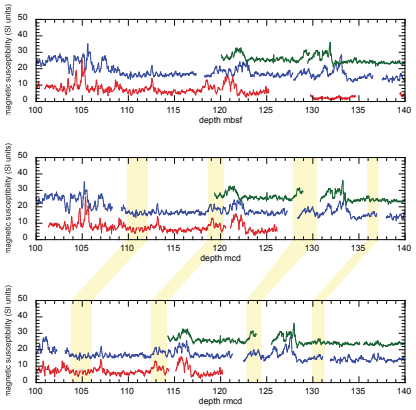

Figure S2C. Magnetic susceptibility (MS) of holes 1258A (red), 1258 B (blue), and 1258C (green) plotted along shipboard mbsf (top panel), shipboard composite depth (mcd, middle panel), and revised composite depth (rmcd, lower panel). The yellow shaded areas highlight major changes between mcd and rmcd. Note: MS values of Hole 1258B and 1258 C are offset by 10 and 20 units, respectively, for clarity.

Fig. 3.

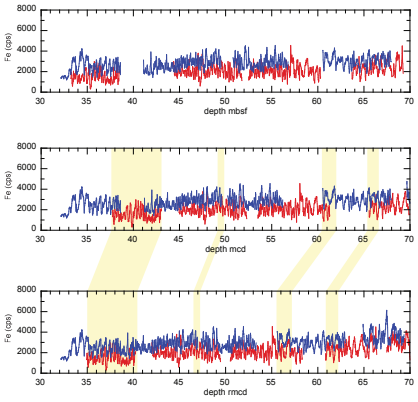

Figure S3A. XRF core scanning iron (Fe) intensity records of holes 1258A (red) and 1258B (blue) plotted along shipboard mbsf (top panel), shipboard composite depth (mcd, middle panel), and revised composite depth (rmcd, lower panel). The yellow shaded areas highlight major changes between mcd and rmcd. Note: MS values of Hole 1258B are offset by 10 units for clarity.

Fig. 4.

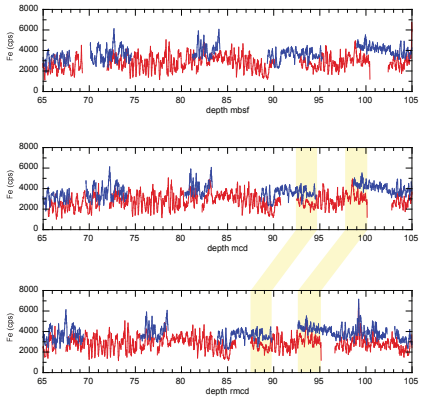

Figure S3B. XRF core scanning iron (Fe) intensity records of holes 1258A (red) and 1258B (blue) plotted along shipboard mbsf (top panel), shipboard composite depth (mcd, middle panel), and revised composite depth (rmcd, lower panel). The yellow shaded areas highlight major changes between mcd and rmcd. Note: MS values of Hole 1258B are offset by 10 units for clarity.

Fig. 5.

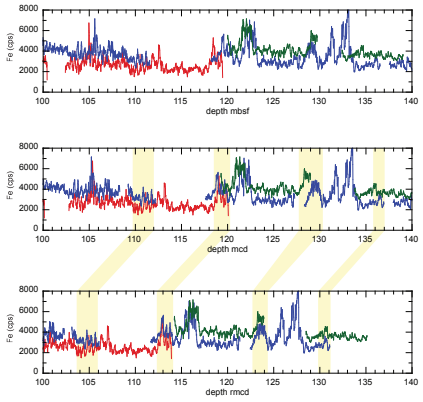

Figure S3C. XRF core scanning iron (Fe) intensity records of holes 1258A (red), 1258 B (blue), and 1258C (green) plotted along shipboard mbsf (top panel), shipboard composite depth (mcd, middle panel), and revised composite depth (rmcd, lower panel). The yellow shaded areas highlight major changes between mcd and rmcd. Note: MS values of Hole 1258B and 1258 C are offset by 10 and 20 units, respectively, for clarity.

Fig. 6.

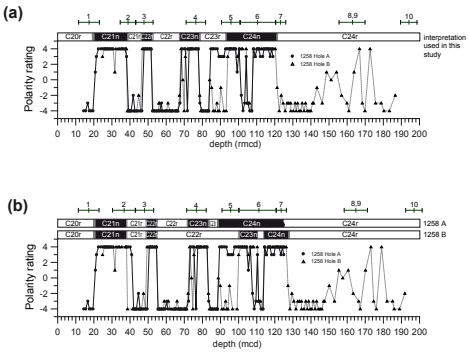

Figure S4. Polarity rating scheme of the inclination data from ODP Holes 1258A (triangles) and B (dots) (Suganuma and Ogg, 2006) with the paleomagnetic reversal pattern interpretation of this study (a) and the original interpretation (b) of Suganuma and Ogg (2006). Please note that (a) is plotted on the revised composite depth (rmcd) skale and (b) is plotted against the shipboard composite depth (mcd). The magnetostratigraphy of ODP Site 1258 in relation to the revised composite depth (rmcd) is given in Table S6. For details of the polarity rating scheme see Suganuma and Ogg (2006). Legends for nannofossil datums from Hole 1258A (Shipboard Scientific Party 2004): 1 LO *N. fulgens*, 2 HO *D. sublodoensis*, 3 HO *D. lodoensis*, 4 HO *T. orthostylus*, 5 LO *D. lodoensis*, 6 LO *S. radians*, 7 LO *T. orthostylus*, 8 LO *D. diastypus*, 9 HO *D. multiradiatus*, 10 HO *Fasciculitus spp.*.

Fig. 7.